Available online at www.sciencedirect.com
SCIENCE DIRECT®
ELSEVIER
International Journal of Solids and Structures 42 (2005) 4971–4987
INTERNATIONAL JOURNAL OF SOLIDS and STRUCTURES
www.elsevier.com/locate/ijsolstr

Improved parameter identification using additional spectral information

Dongho Nam [a], Sanghyun Choi [b,*], Sooyong Park [c], Norris Stubbs [d]

[a] *Dannenbaum Engineering Corp., 3100 W. Alabama, Houston, TX 77098, USA*
[b] *Structural Systems and Site Evaluation Department, Korea Institute of Nuclear Safety, Guseong-Dong, Yuseong-Gu, Daejeon 305-600, Republic of Korea*
[c] *School of Architecture, Youngsan University, Junam-Ri, Ungsang-Up, Yangsan-Si, Kyungnam 626-847, Republic of Korea*
[d] *Department of Civil Engineering, Texas A&M University, College Station, TX 77843, USA*

Received 28 September 2004; received in revised form 10 February 2005
Available online 19 March 2005

Abstract

Spectral information such as natural frequencies from a frequency response function has been widely utilized in structural parameter identification problems. Recently the use of other information in the frequency response function, e.g., antiresonant frequencies, is getting attention. This paper presents application of additional spectral information such as antiresonant frequencies and static compliance dominant frequencies to structural parameter identification problems. The existing sensitivity-based system identification technique is extended by adopting the antiresonant frequencies and the static compliance dominant frequencies, and the performance of the approach using additional spectral information is compared with the approach using only natural frequencies via a numerical example of a mechanical system. The results of the numerical study indicate that the use of additional spectral information improves the accuracy in parameter identification.
© 2005 Elsevier Ltd. All rights reserved.

Keywords: Structural parameter identification; Natural frequency; Antiresonant frequency; Static compliance dominant frequency

* Corresponding author. Fax: +82 42 868 0523.
E-mail addresses: sidnde@naver.com (D. Nam), schoi@kins.re.kr (S. Choi), sypark@ysu.ac.kr (S. Park), n-stubbs@tamu.edu (N. Stubbs).

0020-7683/$ - see front matter © 2005 Elsevier Ltd. All rights reserved.
doi:10.1016/j.ijsolstr.2005.02.017

1. Introduction

There exists an increasing need for reliable and efficient nondestructive methods to identify structural parameters (e.g. stiffness, mass, or damping) and to assess the structural integrity of such critical structures as aerospace structures, offshore structures, buildings, and bridges. To date, a corpus of interdisciplinary knowledge from physics, mathematics, materials science, applied mechanics, and computer engineering have coalesced to provide reliable nondestructive evaluation for monitoring the health of critical structures. However, nondestructive evaluation would have been an empty promise if applied identification methods were not reliable enough to obtain the confidence level needed to make structural safety or useful life decisions. Even with many system identification (SI) techniques and nondestructive damage evaluation (NDE) algorithms developed to date (Doebling et al., 1996), the SI and the NDE procedures for complex structural systems still present many problems, and improving generality and reliability of the SI and the NDE are paramount and one of the more pressing problems in the civil engineering field (Farrar and Jauregui, 1996). In an attempt to resolve these issues, this paper focuses on the performance improvement in the SI, aspect of the problem namely the parameter identification, by utilizing additional spectral information.

System identification is defined as the determination, on the basis of input and output, of the characteristics or properties of a system within a specified class of systems to which it is equivalent (Zadeh, 1962). The process of SI consists of three main steps: (1) defining a model and planning some experiments to measure the response of the system (model selection and testing); (2) using the given model and the measured response to estimate the unknown parameters of the model (parameter estimation); and (3) validating and refining the model (model validation or model updating). In structural mechanics, the parameter estimation has been used to identify the structural parameters and consequently to evaluate the modal parameters (e.g. resonant frequencies, mode shapes, and modal damping) which define the behavior of a structural system. The identified parameters obtained using SI techniques for structures can then be applied to the problems of NDE, and the assessment of structural degradation and deterioration that can reduce the useful life and safety of structures.

The spectral quantities usually utilized in SI techniques are natural frequencies, modeshapes, and frequency response functions (FRF). However, in real application, only a few frequencies can be extracted with acceptable accuracy, and measured modeshapes and FRFs are usually accurate to within 10% at best (Friswell and Mottershead, 1995). Also, even though the direct use of FRF in SI problems can simplify modal analysis procedures, it requires extensive computational efforts (Mottershead, 1990; Lin and Ewins, 1994). These limitations motivated the introduction of other quantities in the FRF to be utilized in the problem of identifying structural systems. One such addition is the antiresonant frequencies. The main advantage of the use of antiresonances is that the antiresonances are located along the frequency axis and can be easily and accurately measurable like natural frequencies.

To date, the antiresonant frequencies have been applied to several engineering problems. Lallement and Cogan (1992) suggested the use of antiresonant frequencies in addition to natural frequencies and mode shapes to identify structural systems. Kajiwara and Nagamatsu (1993) proposed sensitivity analysis using natural frequencies and antiresonant frequencies for structural dynamic optimization problems. The proposed approach was applied to determine the optimum thickness of a plate in order to eliminate resonance peaks from the FRF. Gao and Randall (1996) proposed a procedure to extract poles and zeros of transfer functions from response vibrations. In addition, the procedure for regeneration of updated FRFs could be used in an inverse filtering process to obtain better estimates of the forcing functions than would result from assuming no change in the structural properties. Mottershead (1998) demonstrated that the sensitivities of the antiresonant frequencies could be expressed as a linear combination of the sensitivities of the natural frequencies and the mode shapes. Another useful finding was that if closely predicted natural frequencies and mode shapes failed to converge together with the antiresonant frequencies onto measured values then it had to be concluded that the analytical model could not represent the physical system under test. D'Ambrogio and Fregolent (1998) utilized the antiresonances for model validation via force residual updating—

interactive technique (FRU-IT) since the antiresonant frequencies can reduce the influence of measurement errors that cause the ill-conditioning of the system identification problem. Moreover, it was shown that antiresonance information is not independent of mode shape information, which is preferable for two reasons: (1) antiresonant frequencies can be identified from experimental FRFs with much less error than mode shapes and (2) correlation between experimental and analytical antiresonances is a good index of the correlation between experimental and analytical FRFs. Wahl et al. (1999) discussed the resonance–antiresonance behavior of FRFs for lightly damped linear systems in experimental structural analysis. Based on the FRF measurements of structures supported arbitrarily, it was possible to determine the natural frequencies of structures under ideal boundary conditions that were impossible to obtain in laboratory tests. They concluded that the properties of antiresonances might lead to future applications in different fields of structural engineering such as system identification and location of structural faults. The antiresonant frequencies have also been applied in the problems of model updating (Rade et al., 1996; Jons and Turcotte, 2002) and crack detection (Dilena and Morassi, 2004; Douka et al., 2004). However, the use of antiresonant frequencies to SI problems is still in its early stage and the applicability to various SI techniques has not been fully investigated. Finally, so far no attempt has been made to utilize other information from a FRF than natural and antiresonant frequencies.

In this paper, the use of additional information from an FRF including antiresonant frequencies and other information, e.g., the static compliance dominant (SCD) frequencies (Nam, 2001), to a parameter identification problem is investigated. The SCD frequencies are the frequencies that yield the same static compliances of the structural system on the FRF. The possible use of the additional spectral information to the parameter identification problem is explored using a sensitivity-based SI technique. The following steps are performed: (1) additional spectral information that can be possibly utilized in developing more accurate and effective SI techniques is introduced; (2) a sensitivity-based SI technique is extended to accommodate the additional spectral information and (3) numerical studies are conducted on a mechanical model to investigate the performance of parameter identification using additional information from an FRF, i.e., natural frequencies, antiresonant frequencies, and SCD frequencies.

2. Additional spectral information

At a given frequency, ω, the FRF, $\mathbf{H}(\omega)$, incorporates not only information about the structural parameters of the system but also about the force function. The available information at a set of frequencies (e.g. natural frequencies) in the FRF can be defined as spectral information. An important feature that arises from the FRF is that the system output will inevitably contain spectral contents that do not appear in the time domain analysis. In that regard, any value in an FRF, $\mathbf{H}(\omega)$, can be defined as potential spectral information. However, to be applicable to identification problems, the spectral information has to satisfy the following requirements: (1) the information has to be easily and consistently extractable; (2) the information has to effectively reflect the changes in the structural properties of the system; and (3) the information can be extracted with acceptable accuracy.

In this paper, two types of spectral information, antiresonant frequencies and SCD frequencies, are selected. The antiresonant frequencies are associated with the dips in the magnitude of the FRF, while the natural frequencies are the peaks in the magnitude of the FRF. The frequencies that yield the same static compliances of the structural system on the FRF can be defined as SCD frequencies.

2.1. Antiresonant frequencies

Antiresonant frequencies can be obtained from either experimental or analytical FRFs. The FRF matrix, $\mathbf{H}(\omega)$, can be written in terms of the determinants of the dynamic stiffness matrix as (Ewins, 1984)

$$\mathbf{H}(\omega) = \mathbf{f}/\mathbf{u} = (\mathbf{k} - \omega^2\mathbf{m})^{-1} = \frac{\mathrm{adj}(\mathbf{k} - \omega^2\mathbf{m})}{\det(\mathbf{k} - \omega^2\mathbf{m})} \tag{1}$$

where $\mathbf{m}$ and $\mathbf{k}$ are the $(n \times n)$ mass and stiffness matrices, respectively; $\mathbf{f}$ and $\mathbf{u}$ are the $(n \times 1)$ force and displacement vectors of the structural system, respectively; and adj( ) and det( ) are the adjoint and the determinant matrices, respectively. The i–jth components of the FRF can be rewritten in terms of modeshapes as

$$\mathbf{H}_{ij}(\omega) = \sum_{k=1}^{n} \frac{\mathbf{\Phi}_{ik}\mathbf{\Phi}_{jk}}{(\lambda_k - \omega^2)} \tag{2}$$

where λ_k is the kth eigenvalue, and $\mathbf{\Phi}_{ik}$ and $\mathbf{\Phi}_{jk}$ are the elements i and j of the kth mode shape vector.

To obtain antiresonant frequencies from experimental FRFs, there are two available methods: antiresonant frequencies can be achieved by a dip-picking technique that selects the dips from the log magnitude–frequency plot of a given FRF, or antiresonant frequencies can be calculated by a curve-fitting technique using the rational fraction polynomial representation of a given FRF and determining the zeros of the function.

To obtain antiresonant frequencies from analytical FRFs (e.g. from a finite element model), one can calculate the zeroes of the FRF matrix that is the inverse of the dynamic stiffness matrix. By definition, the zeroes of the i–jth FRF occur at frequencies that cause the numerator, $\mathrm{adj}(\mathbf{k} - \omega^2\mathbf{m})$, in (1) to become singular. Also, they can be calculated from the eigenvalue problem as the eigenvalues of $(\mathbf{m}^{-1}\mathbf{k})_{ij}$.

In addition, antiresonant frequencies can be achieved from both point FRFs and transfer FRFs. When any row and its corresponding column (e.g. ith row and column) of the FRF matrix in (1) are removed, which is called the point FRF, the structure is grounded at the ith degree of freedom and its eigenvalues may interlace the eigenvalues of the given original structure. If the removed row and column are different (e.g. ith row and jth column), called the transfer FRF, the physical meaning of the fictitious structure is not clear due to the fact that the FRF matrix is not symmetric. Thus, antiresonant frequencies of the fictitious structure are the zeroes of the modified FRF, $\mathbf{H}_{ij}(\omega)$, which may be either point FRF or transfer FRF, of the given structure with the ith row and jth column deleted (Mottershead, 1998). It should be clear that antiresonant frequencies could be abundant since the zeroes of FRFs occur at different frequencies for different measurement locations.

2.2. Static compliance dominant frequencies

Additional pieces of information from an FRF can be utilized to improve the accuracy of SI techniques. In this study, the SCD frequency is introduced.

From (2), the i–jth transfer FRF can be rewritten as

$$\mathbf{H}_{ij}(\omega) = \sum_{k=1}^{n} \frac{\mathbf{\Phi}_{ik}\mathbf{\Phi}_{jk}}{(\omega_k^2 - \omega^2)} \tag{3}$$

where ω_k is the kth natural frequency. The static compliance can be obtained from (3) with $\omega = 0$ as follows:

$$\mathbf{H}_{ij}(0) = \sum_{k=1}^{n} \frac{\mathbf{\Phi}_{ik}\mathbf{\Phi}_{jk}}{\omega_k^2} \tag{4}$$

For different values of the parameter ω, let a function be defined as

$$\bar{\mathbf{H}}_{ij}(\omega) = \sum_{k=1}^{n} \frac{\mathbf{\Phi}_{ik}\mathbf{\Phi}_{jk}}{(\omega_k^2 - \omega^2)} - \sum_{k=1}^{n} \frac{\mathbf{\Phi}_{ik}\mathbf{\Phi}_{jk}}{\omega_k^2} \tag{5}$$

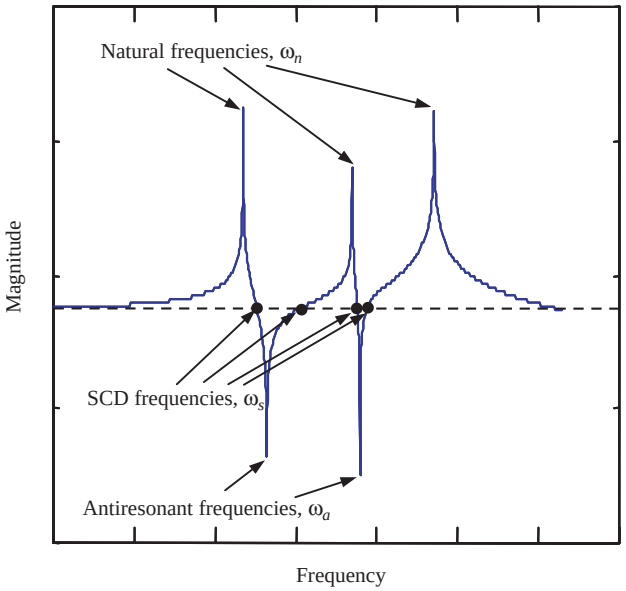

Fig. 1. Graphical representation of natural, antiresonant, and SCD frequencies.

Then, roots of (5) can be found by setting the whole expression equals to zero.

$$\bar{\mathbf{H}}_{ij}(\omega) = 0 \tag{6}$$

The positive roots of (6) are the frequencies of the *i–j*th transfer FRF that can yield the same static compliances of the structural system. Those frequencies are defined as SCD frequencies in this study. The graphical representations of the SCD frequencies are depicted in Fig. 1 along with the natural and antiresonant frequencies. In Fig. 1, the corresponding frequencies to the dots represent the SCD frequencies, while the peaks and the dips correspond to the resonant and the antiresonant frequencies, respectively. The SCD frequencies can be extracted from experimental data by selecting the frequency values from the magnitude plot of the FRF at $\omega = 0$.

3. System identification theory

Sensitivity type methods have gained acceptance due to their ability to reconstruct the correct measured resonant frequencies and mode shapes. Almost all sensitivity-based methods utilize a sensitivity matrix based on the partial derivatives of modal parameters with respect to structural parameters. During the identification process, the analytical mass and stiffness matrices of a structural system are updated. An updated eigensolution is obtained and the same process is repeated until the results are satisfied within a predetermined tolerance. It should be noted that the formulation of the sensitivity matrix is based on a Taylor's series expansion and hence the method is an approximate one. In general, sensitivity-type methods depend on the selection of parameters and the definition of the optimization constraints. For instance, the parameters can be elements of the mass and stiffness matrices. Sensitivity-based methods provide an updated analytical model capable of reproducing the measured modal parameters, but they have the drawback of modifying only the most sensitive elements. A sensitivity-type method that utilizes statistics as the basis for model updating was formulated by Collins et al. (1974) to systematically use experimental

measurements of the modal parameters of a structure to modify the stiffness and mass terms of a finite element model of the structure. The sensitivity matrix technique was exploited further in combination with SI and nondestructive damage detection studies by Stubbs (1985).

In this section, a sensitivity-based SI method proposed by Stubbs and Osegueda (1990) is presented and extended to accommodate other spectral information, i.e., antiresonant frequencies and static compliance dominant frequencies.

3.1. Parameter identification algorithm

Let the mathematical model of a system be defined by n scalar parameters x_i in which $i = 1, 2, \ldots, n$. The parameter, x_i, can be collected into the vector $\boldsymbol{x}$. Using Taylor series expansion

$$f(\boldsymbol{x} + \mathrm{d}\boldsymbol{x}) = \sum_{k=0}^{n} \frac{1}{k!} f^{(k)}(\boldsymbol{x}) \mathrm{d}\boldsymbol{x}^k + E_n(\mathrm{d}\boldsymbol{x}) \tag{7}$$

where

$$E_n(\mathrm{d}\boldsymbol{x}) = \frac{1}{(n+1)!} f^{(n+1)}(\xi) \mathrm{d}\boldsymbol{x}^{n+1} \tag{8}$$

in which the point ξ is between $\boldsymbol{x}$ and $\boldsymbol{x} + \mathrm{d}\boldsymbol{x}$. Considering the first term in (7) and assuming that $f(x + \mathrm{d}x)$ represents the true solutions for a real system and that $f(x)$ describes the approximate solutions for a mathematical model, the error, e, can be expressed as

$$e = f(\boldsymbol{x} + \mathrm{d}\boldsymbol{x}) - f(\boldsymbol{x}) = \sum_{i=1}^{n} \frac{\partial f}{\partial x_i} \mathrm{d}x_i \tag{9}$$

If (9) is applied to m functions, the jth expression for the error is given by

$$e_j = \sum_{i=1}^{n} \frac{\partial f_j}{\partial x_i} \mathrm{d}x_i, \quad (j = 1, 2, \ldots, m) \tag{10}$$

Normalizing (10) dividing by f_j yields (Stubbs et al., 1994)

$$\frac{e_j}{f_j} = \sum_{i=1}^{n} \frac{\partial f_j}{\partial x_i} \frac{x_i}{f_j} \frac{\mathrm{d}x_i}{x_i} \tag{11}$$

or

$$z_j = \sum_{i=1}^{n} f_{ji} \alpha_i \tag{12}$$

where $z_j = \frac{e_j}{f_j}$; $\alpha_i = \frac{\mathrm{d}x_i}{x_i}$; and $f_{ji} = \frac{\partial f_j}{\partial x_i} \frac{x_i}{f_j}$, representing the jth fractional change of the solution vectors between real and mathematical system, the ith fractional changes of the scalar parameters, and the jth sensitivities with respect to the ith scalar parameters, respectively. Eq. (12) can be rewritten in matrix form as

$$\mathbf{Z} = \mathbf{F}\boldsymbol{\alpha} \tag{13}$$

The vector $\mathbf{Z}$ is obtained from the differences in results for a real and a mathematical system. The gradient of f, the scalar parameters x, and the solution of the function f determine the sensitivity matrix $\mathbf{F}$. The vector $\boldsymbol{\alpha}$ is the only unknown to estimate, e.g., stiffness, mass, or damping. Note that, in this paper, only changes in stiffness parameters are considered in $\boldsymbol{\alpha}$, because in structural parameter identification problems: (1) the change in masses is negligible in common structural damage (e.g., cracks, time-dependent stiffness

degradation in concrete structure, delamination in composite structures, loosen connections in steel structures); and (2) the effect of changes in damping parameters on changes in spectral information (e.g., natural frequencies) is negligibly small (Farrar and Jauregui, 1996).

The vector $\mathbf{Z}$ includes Z_n, Z_a, and Z_s that represent the fractional change in the square of the natural frequencies, the antiresonant frequencies, and the SCD frequencies, respectively.

$$\mathbf{Z} = \{ Z_n \quad Z_a \quad Z_s \}^{\mathrm{T}} \tag{14}$$

or

$$Z = \left\{ z_{n1} \;\; z_{n2} \;\; \cdots \;\; z_{ni} \;\; \cdots \;\; z_{nm} : z_{a1} \;\; z_{a2} \;\; \cdots \;\; z_{aj} \;\; \cdots \;\; z_{an} : z_{s1} \;\; z_{s2} \;\; \cdots \;\; z_{sk} \;\; \cdots \;\; z_{sp} \right\}^{\mathrm{T}}$$
$$(i = 1, 2, \ldots, m; \;\; j = 1, 2, \ldots, n; \;\; k = 1, 2, \ldots, p) \tag{15}$$

where i, j, and k represent the number of natural frequencies, antiresonant frequencies, and static compliance dominant frequencies available, respectively, and z_{ni} , z_{aj}, z_{sk} are the fractional change in the ith natural frequency, the fractional change in the jth antiresonant frequency, and the fractional change in the kth SCD frequency given by

$$z_{ni} = \frac{\bar{\omega}_{ni}^2 - \omega_{ni}^2}{\omega_{ni}^2}, \quad z_{aj} = \frac{\bar{\omega}_{aj}^2 - \omega_{aj}^2}{\omega_{aj}^2}, \quad z_{sk} = \frac{\bar{\omega}_{sk}^2 - \omega_{sk}^2}{\omega_{sk}^2} \tag{16}$$

where ω_{ni} is the measured natural frequency; $\bar{\omega}_{ni}$ is the corresponding value for the initial structure; ω_{aj} is the measured antiresonant frequency; $\bar{\omega}_{aj}$ is the corresponding value for the initial structure; ω_{sk} is the measured SCD frequency and $\bar{\omega}_{sk}$ is the corresponding value for the initial structure.

From (13), it can be deduced that the fractional change in structural stiffness, α, may be expressed by

$$\boldsymbol{\alpha} = \mathbf{F}^{-1}\mathbf{Z} = \mathbf{F}^{-1} \begin{Bmatrix} Z_n \\ Z_a \\ Z_s \end{Bmatrix} \tag{17}$$

where $\mathbf{Z}$ is the $(m+n+p)\times 1$ column matrix, $\mathbf{F}$ is the $(m+n+p)\times q$ matrix, and $\boldsymbol{\alpha}$ is the $(q\times 1)$ column matrix when there are q unknown structural parameters to be identified.

For an underdetermined system that involves more unknowns than equations (i.e., $(m+n+p) < q$), the rectangular matrix $\mathbf{F}$ does not have an inverse. A partial replacement for the inverse is provided by the Moore–Penrose pseudoinvese, which is obtained by

$$\mathbf{F}^{-1} = \mathbf{F}^{\mathrm{T}}(\mathbf{F}\mathbf{F}^{\mathrm{T}})^{-\mathbf{1}} \tag{18}$$

In a similar way, the pseudoinverse of a rectangular matrix $\mathbf{F}$ for an overdetermined system (i.e., $(m+n+p) > q$) is given by

$$\mathbf{F}^{-1} = (\mathbf{F}^{\mathrm{T}}\mathbf{F})^{-1}\mathbf{F}^{\mathrm{T}} \tag{19}$$

It should be noted that the solution obtained by (18) is the minimal norm solution and may not be unique.

3.2. Updating algorithm

The relationship between the fractional stiffness change and the stiffness parameters for the jth element is defined as (Choi and Stubbs, 2004)

$$\alpha_j = \frac{\Delta k_j}{k_j} \tag{20}$$

where $\Delta k_j = k_j^* - k_j$; k_j^* is the unknown stiffness parameter of the jth element of the existing structure; and k_j is the known stiffness parameter of the jth element of the initial structure. Eq. (20) can be rewritten as

$$k_j^* = k_j(1 + \alpha_j) \tag{21}$$

where α_j is the fractional change in stiffness of the jth element.

Suppose that the corresponding sets of m resonant frequencies, n antiresonant frequencies, and p SCD frequencies of the initial FE model and the existing structure are known. Before implementing (17) to get the fractional stiffness changes of q elements between the initial and the existing structures, the sensitivity matrix, **F**, should first be developed. The sensitivity matrix represents the relation between fractional changes in stiffness and fractional changes in the frequencies of two structures.

The following procedure can be used to determine the sensitivity matrix: first, m resonant frequencies are numerically generated for the initial FE model of a system; second, n antiresonant frequencies and p SCD frequencies are computed from the FRF of the FE model using (1) and (6); third, a known fractional stiffness change, α_j at element j of the FE model is introduced and the corresponding m resonant frequencies are numerically generated; fourth, based on a known parameter, α_j, at element j of the FE model, n antiresonant frequencies and p SCD frequencies are computed from the FRF such as the second step; fifth, the fractional changes between the $(m + n + p)$ initial frequencies and the $(m + n + p)$ frequencies corresponding to the parameter α_j are computed using (16); sixth, each component of the jth column of the matrix **F** is computed dividing the fractional changes in each frequency by the simulated severity at the element j; and finally, the $(m + n + p) \times q$ matrix **F** is generated repeating the procedure for all q elements.

With the **F** matrix obtained, the following 8-step algorithm is proposed to identify a target structure

1. Extract FRFs and natural frequencies from the target structure (i.e. an existing structure).
2. Compute the antiresonant frequencies and the SCD frequencies of the target structure.
3. Select an initial FE model of the structure utilizing all possible knowledge about the design and construction of the structure.
4. Compute the natural frequencies, the antiresonant frequencies and the SCD frequencies of the initial FE model.
5. Compute the sensitivity matrix, **F**, for the FE model.
6. Compute the fractional changes in frequencies between the FE model and the target structure.
7. Fine-tune the FE model by first solving (17) to estimate stiffness changes and next solving (21) to update stiffness parameters of the FE model.
8. Repeat steps 1–7 until $\mathbf{Z} \approx 0$ or $\boldsymbol{\alpha} \approx 0$ when the structural parameters of the FE model are identical to the existing target structure.

4. Verification

Using simulated data from a simple mechanical system, the performance of the proposed parameter identification method using the additional spectral information, i.e., antiresonant frequencies and SCD frequencies, is investigated. The mechanical model selected here to evaluate the methodology is shown in Fig. 2. The three-degree-of-freedom, undamped, mechanical system consists of three unequal masses, m_i $(i = 1, 2, 3)$, that are interconnected and anchored to their supports by six linear spring elements, k_i $(i = 1, 2, \ldots, 6)$. The stiffnesses, masses, and the material properties of the model are listed in Table 1. In this study, the masses of the model are assumed to be known and thus the six stiffness parameters of the system are the only elements to be identified.

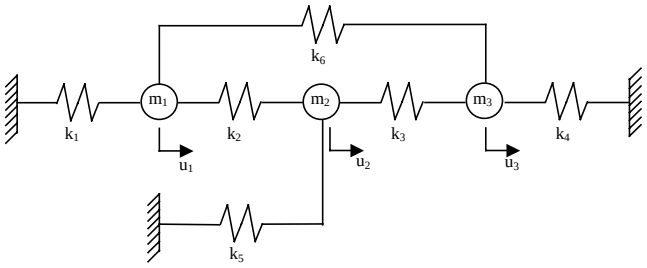

Fig. 2. Configuration of the mechanical system.

Table 1
Material properties of the mechanical system

	Element					
Stiffness	k_1	k_2	k_3	k_4	k_5	k_6
	2	1	1	2	2	1
Mass	m_1		m_2		m_3	
	0.8		2.0		1.2	

For following initial values of the structural properties are assumed:

(1) Case 1—the initial assumed stiffnesses are 10% less than the true stiffnesses
(2) Case 2—the initial assumed stiffnesses are 20% less than the true stiffnesses
(3) Case 3—the initial assumed stiffnesses are 50% less than the true stiffnesses

These three cases are selected to demonstrate the rate of convergence and the accuracy of the prediction as a function of the distance of the initial guesses from the true values. The spectral information of the unperturbed system and the three initial systems are summarized in Table 2.

The system identification procedure defined in the previous section was performed to identify the structural stiffness parameters of the system. First, the identification was performed with 3 natural frequencies. The results can be seen in Tables 3–5. The results show that the maximum errors in the estimated structural parameters for Case 1, Case 2, and Case 3 are 1.81%, 3.56%, and 8.93%, respectively. Figs. 3 and 4 show the magnitude and phase plots of the FRF for the system with the identified stiffness and the true stiffness for Case 3. In Figs. 3 and 4, it is shown that the antiresonant frequencies of the system do not match up even though the natural frequencies fit.

To investigate the performance of the parameter identification including additional spectral information, numerical simulation sets were conducted using the following combination of natural frequencies and antiresonant frequencies, and/or SCD frequencies: (1) Group 1—natural frequencies and antiresonant frequencies from point FRFs (utilizing 5, 7, and 9 pieces of data); (2) Group 2—natural frequencies and antiresonant frequencies from transfer FRFs (utilizing 4, 5, and 6 pieces of data); (3) Group 3—natural frequencies and antiresonant frequencies from point and transfer FRFs (utilizing 12 pieces of data); (4) Group 4—natural frequencies and static compliance dominant frequencies (utilizing 5 and 9 pieces of data); and (5) Group 5—natural frequencies, antiresonant frequencies, and static dominant frequencies (utilizing 7 pieces of data).

In Group 1, 5 pieces of information consisting of 3 natural frequencies and 2 antiresonant frequencies obtained from the point FRF (H_{11}); 7 pieces of information consisting of 3 natural frequencies and 4 antiresonant frequencies obtained from two point FRFs (H_{11} and H_{22}); and 9 pieces of information consisting

Table 2
Natural frequencies and additional spectral information of the mechanical system

	Mode	Frequency (rad/s)			
		Target	Case 1	Case 2	Case 3
Natural frequency	1	1.173	1.113	1.049	0.830
	2	1.848	1.753	1.653	1.306
	3	2.354	2.234	2.106	1.665
Antiresonant frequencies from point FRFs	1–2 (H_{11})	1.319	1.251	1.179	0.932
	2–3 (H_{11})	1.896	1.799	1.696	1.314
	1–2 (H_{22})	1.688	1.601	1.510	1.194
	2-3 (H_{22})	2.342	2.222	2.095	1.656
	1–2 (H_{33})	1.343	1.274	1.201	0.950
	2–3 (H_{33})	2.279	2.162	2.039	1.612
Antiresonant frequencies from transfer FRFs	1–2 (H_{12})	2.041	1.936	1.826	1.443
	1–3 (H_{13})	1.581	1.500	1.414	1.118
	2–3 (H_{23})	2.500	2.372	2.236	1.768
SCD frequencies from point FRFs	1–2 (H_{11})	1.253	1.189	1.121	0.886
	2–3 (H_{11})	1.878	1.782	1.680	1.328
	1–2 (H_{22})	1.494	1.417	1.336	1.056
	2–3 (H_{22})	2.041	1.937	1.826	1.443
	1–2 (H_{33})	1.276	1.210	1.141	0.903
	2–3 (H_{33})	2.182	2.070	1.952	1.544

Table 3
Comparison of identified structural parameters for Case 1

	Pieces of information		Element stiffness (lb/in)						Max. error (%)
			k_1	k_2	k_3	k_4	k_5	k_6	
SI	3	NF	2.034	0.986	0.992	2.036	1.976	0.987	1.81
SI using additional spectral information	5	NF and AF from point FRFs	1.998	1.006	0.991	2.019	1.992	0.997	0.95
	7		2.000	1.000	1.000	2.000	2.000	1.000	0.00
	9		2.000	1.000	1.000	2.000	2.000	1.000	0.00
	4	NF and AF from transfer FRFs	2.036	0.988	0.991	2.034	1.997	0.986	1.69
	5		2.023	0.991	1.007	1.991	1.997	0.993	1.16
	6		2.000	1.000	1.000	2.000	2.000	1.000	0.00
	12	NF and AF from point and transfer FRFs	2.000	1.000	1.000	2.000	2.000	1.000	0.00
	5	NF and SCDF from point FRFs	1.998	1.006	0.991	2.019	1.992	0.997	0.93
	9		2.000	1.000	1.000	2.000	2.000	1.000	0.00
	7	ASI	2.000	1.000	1.000	2.000	2.000	1.000	0.00
True element stiffness			2.000	1.000	1.000	2.000	2.000	1.000	

NF—natural frequencies, AF—antiresonant frequencies; SCDF—static compliance dominant frequencies; ASI—additional spectral information.

of 3 natural frequencies and 6 antiresonant frequencies obtained from three point FRFs (H_{11}, H_{22}, and H_{33}). In Group 2, 4 pieces of information consisting of 3 natural frequencies and 1 antiresonant frequencies obtained from the transfer FRF (H_{12}); 5 pieces of information consisting of 3 natural frequencies and 2 antiresonant frequencies obtained from two transfer FRFs (H_{12} and H_{13}); and 6 pieces of information consisting of 3 natural frequencies and 3 antiresonant frequencies obtained from three transfer FRFs (H_{12}, H_{13},

Table 4
Comparison of identified structural parameters for Case 2

	Pieces of information		Element stiffness (lb/in)						Max. error (%)
			k_1	k_2	k_3	k_4	k_5	k_6	
SI	3	NF	2.069	0.972	0.983	2.071	1.955	0.975	3.56
SI using additional spectral information	5	NF and AF from point FRFs	1.996	1.011	0.982	2.038	1.985	0.993	1.91
	7		2.000	1.000	1.000	2.000	2.000	1.000	0.00
	9		2.000	1.000	1.000	2.000	2.000	1.000	0.00
	4	NF and AF from transfer FRFs	2.072	0.976	0.982	2.068	1.955	0.972	3.16
	5		2.046	0.983	1.013	1.983	1.994	0.986	2.32
	6		2.000	1.000	1.000	2.000	2.000	1.000	0.00
	12	NF and AF from point and transfer FRFs	2.000	1.000	1.000	2.000	2.000	1.000	0.00
	5	NF and SCDF from point FRFs	1.998	1.007	0.989	2.024	1.990	0.996	1.18
	9		2.000	1.000	1.000	2.000	2.000	1.000	0.00
	7	ASI	2.000	1.000	1.000	2.000	2.000	1.000	0.00
True element stiffness			2.000	1.000	1.000	2.000	2.000	1.000	

NF—natural frequencies, AF—antiresonant frequencies; SCDF—static compliance dominant frequencies; ASI—additional spectral information.

Table 5
Comparison of identified structural parameters for Case 3

	Pieces of information		Element stiffness (lb/in)						Max. error (%)
			k_1	k_2	k_3	k_4	k_5	k_6	
SI	3	NF	2.179	0.928	0.951	2.178	1.900	0.937	8.93
SI using additional spectral information	5	NF and AF from point FRFs	1.989	1.028	0.954	2.097	1.962	0.983	4.84
	7		2.000	1.000	1.000	2.000	2.000	1.000	0.00
	9		2.000	1.000	1.000	2.000	2.000	1.000	0.00
	4	NF and AF from transfer FRFs	2.183	0.935	0.950	2.173	1.899	0.932	8.63
	5		2.117	0.956	1.034	1.959	1.987	0.965	5.89
	6		2.000	1.000	1.000	2.000	2.000	1.000	0.00
	12	NF and AF from point and transfer FRFs	2.000	1.000	1.000	2.000	2.000	1.000	0.00
	5	NF and SCDF from point FRFs	1.989	1.028	0.953	2.099	1.962	0.982	4.93
	9		2.000	1.000	1.000	2.000	2.000	1.000	0.00
	7	ASI	2.000	1.000	1.000	2.000	2.000	1.000	0.00
True element stiffness			2.000	1.000	1.000	2.000	2.000	1.000	

NF—natural frequencies, AF—antiresonant frequencies; SCDF—static compliance dominant frequencies; ASI—additional spectral information.

and H_{23}). In Group 3, 12 pieces of information consisting of 3 natural frequencies, 6 antiresonant frequencies obtained from three point FRFs (H_{11}, H_{22}, and H_{33}), and 3 antiresonant frequencies obtained from three transfer FRFs (H_{12}, H_{13}, and H_{23}). In Group 4, 5 pieces of information consisting of 3 natural frequencies and 2 SCD frequencies obtained from a point FRF (H_{11}); and 9 pieces of information consisting

of 3 natural frequencies and 6 SCD frequencies obtained from a point FRF (H_{11}, H_{22}, and H_{33}). In Group 5, 7 pieces of information consisting of 3 natural frequencies, 2 antiresonant frequencies obtained from a point FRF (H_{22}), and 2 SCD frequencies obtained from a point FRF (H_{11}).

The system identification results for the 5 groups are summarized in Tables 3–5 for Cases 1–3, respectively. The accuracy of the different parameter identification results are compared via the maximum percentage errors of the identified stiffnesses of the elements, as shown in the tables. From Table 3, while the maximum error in the identified stiffness parameters obtained when using 3 natural frequencies is 1.81%, the maximum errors including additional spectral information are 1.69% when using 4 pieces of information, 1.16% when using 5 pieces of information, and 0% when using more than 6 pieces of infor-

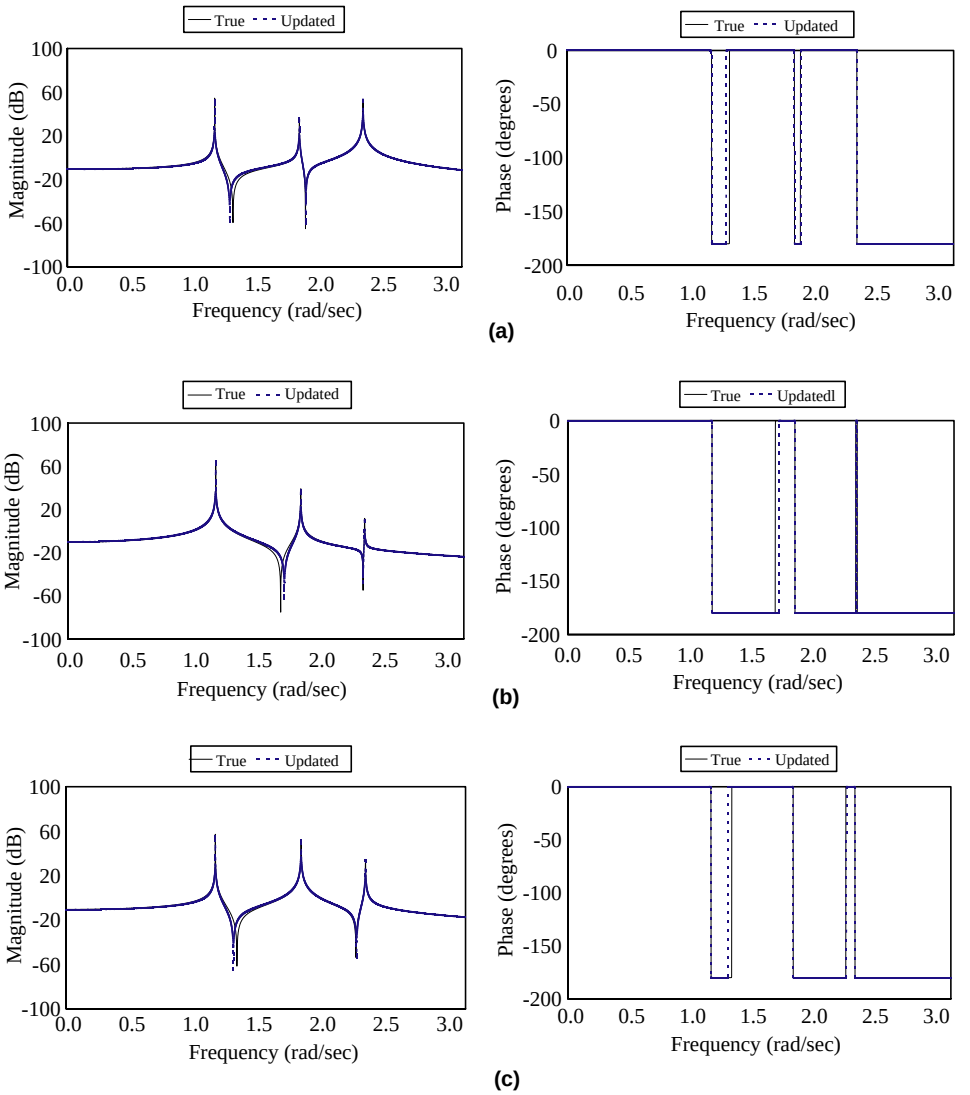

Fig. 3. 12 point FRF amplitude and phase plots for Case 3—using natural frequencies only. (a) FRF and phase plot for H_{11}, (b) FRF and phase plot for H_{22} and (c) FRF and phase plot for H_{33}.

mation. From Table 4, while the maximum error in the identified stiffness parameters obtained when using 3 natural frequencies is 3.56%, the maximum errors including additional spectral information are 3.16% when using 4 pieces of information, 2.32% when using 5 pieces of information, and 0% when using more than 6 pieces of information. From Table 5, while the maximum error in the identified stiffness parameters obtained using 3 natural frequencies is 8.93%, the maximum errors including additional spectral information are 8.63% when using 4 pieces of information, 5.89% when using 5 pieces of information, and 0% when using more than 6 pieces of information. From the tables, it can be also observed that better results could be obtained using the point FRFs than using the transfer FRFs. One notable observation is that, with the addition of the SCD frequencies to the natural frequencies, the accuracy of the stiffness identification is equally effective as using the antiresonant frequencies. These results show that the SCD frequencies can also be utilized in SI problems.

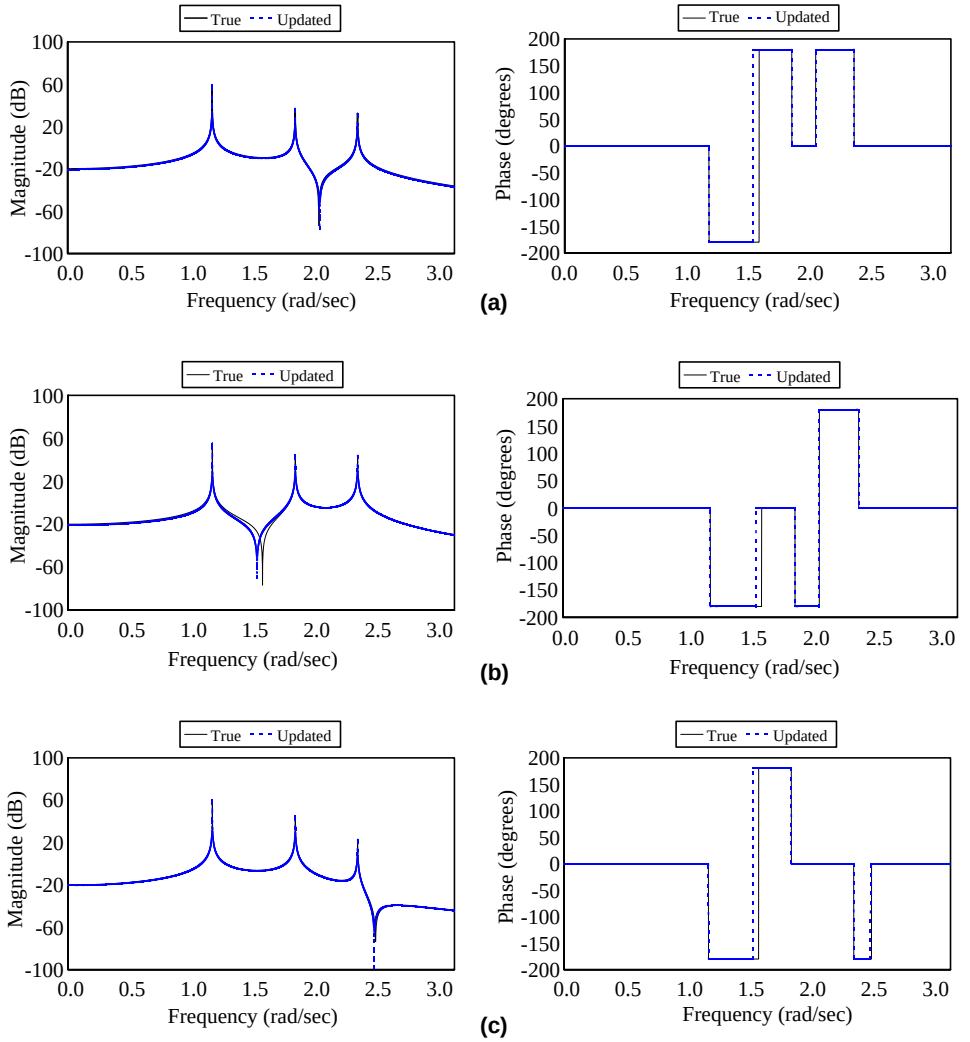

Fig. 4. Transfer FRF amplitude and phase plots for Case 3—using natural frequencies only. (a) FRF and phase plot for H_{12}, (b) FRF and phase plot for H_{13} and (c) FRF and phase plot for H_{23}.

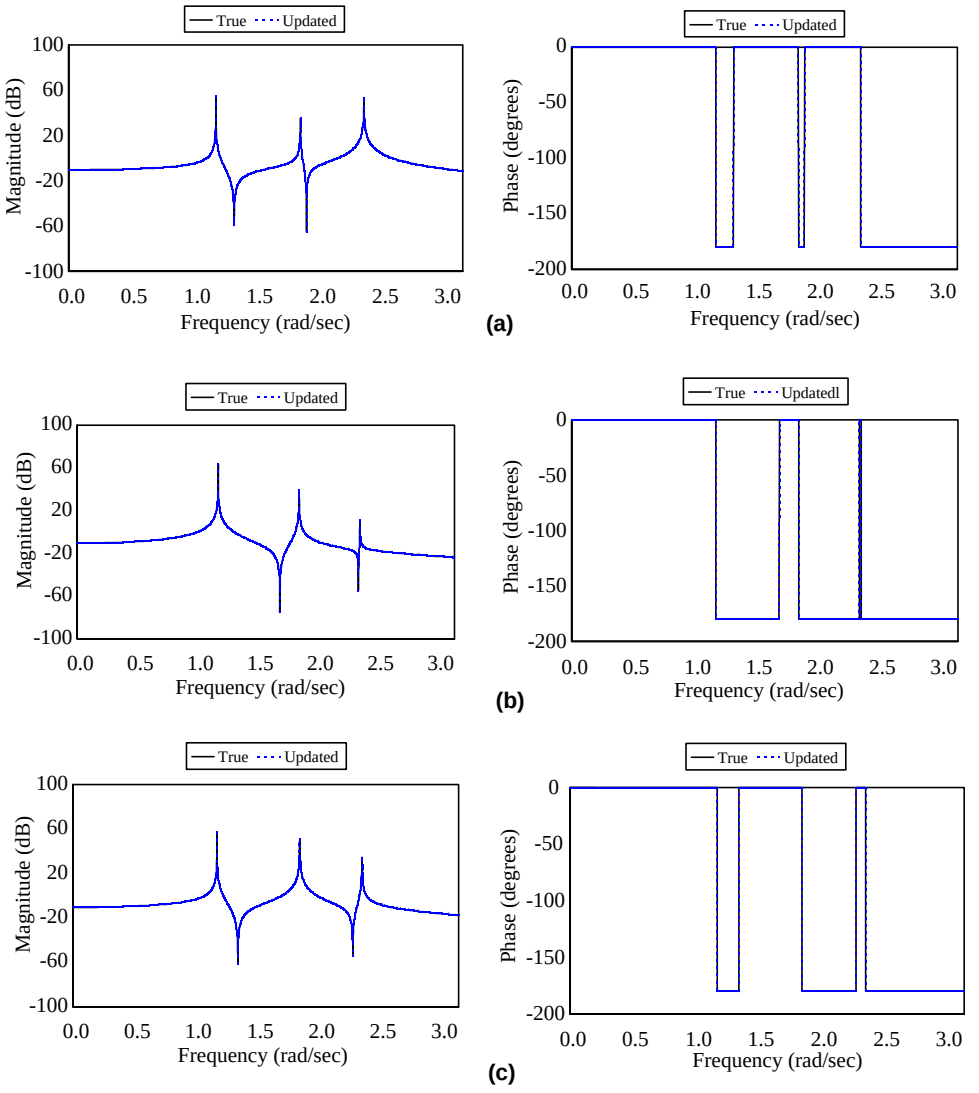

Fig. 5. Point FRF amplitude and phase plots for Case 3—with additional spectral information. (a) FRF and phase plot for H_{11}, (b) FRF and phase plot for H_{22} and (c) FRF and phase plot for H_{33}.

Figs. 5 and 6 show the magnitude and phase plots of the FRFs for the system with the identified stiffness and the true stiffness for Group 1 using 7 pieces of information (3 natural frequencies + 4 antiresonances for point FRFs, H_{11} and H_{22}). To compare with the results using only natural frequencies in Figs. 3 and 4, the results of the same case, Case 3, are depicted. Note that the natural frequencies and antiresonant frequencies of the system match up in Figs. 5 and 6.

5. Discussion

In the preceding section, the improvement in the performance of parameter estimation using additional spectral information was validated via a numerical example of a mechanical system. As expected, with addi-

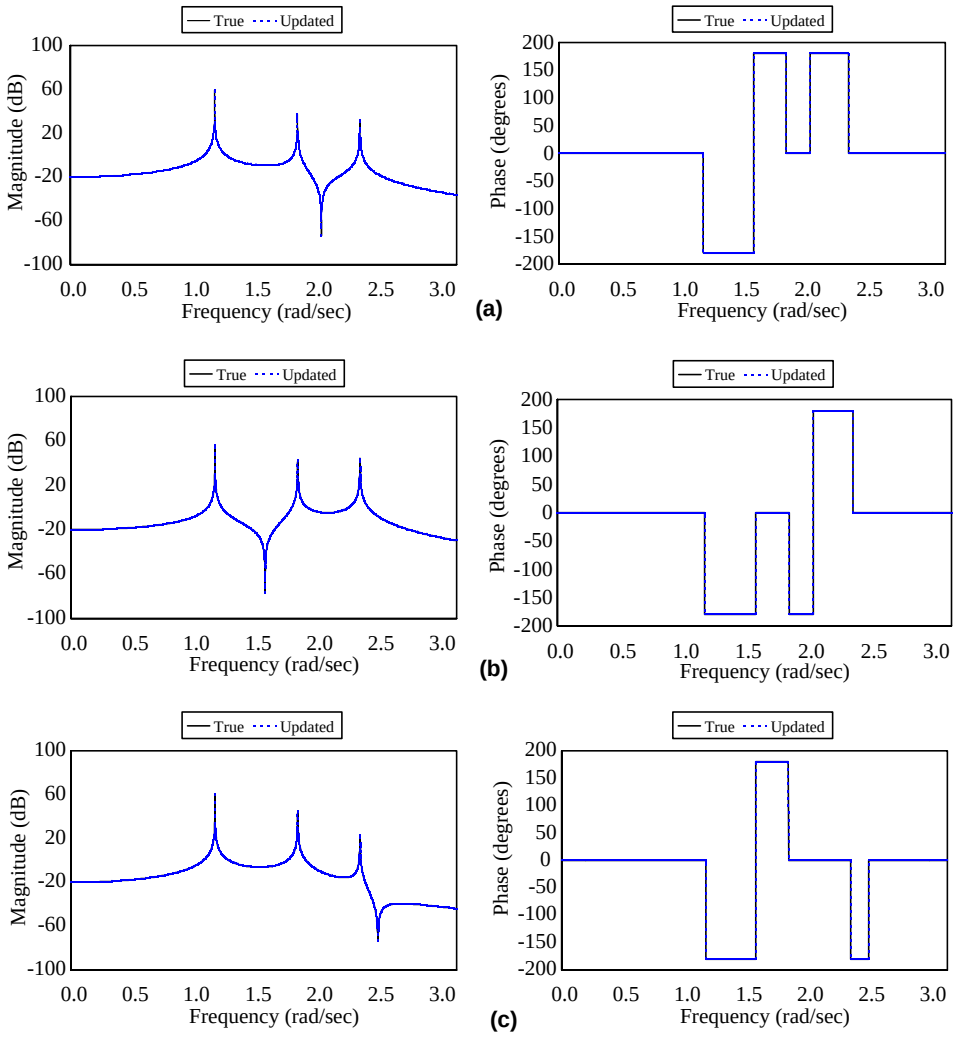

Fig. 6. Transfer FRF amplitude and phase plots for Case 3—with additional spectral information. (a) FRF and phase plot for H_{12}, (b) FRF and phase plot for H_{13} and (c) FRF and phase plot for H_{23}.

tional spectral information, more accurate parameter estimation results can be obtained compared to those using only natural frequencies. Notably, if the number of pieces of spectral information used is equal or greater than the number of stiffness parameters to be identified, the error in the prediction of the stiffness parameters is zero, regardless of the starting point of the iteration. These results suggest that there may be a significant advantage of utilizing additional spectral information in parameter identification problems. In most real-world applications, only a few natural frequencies can be extracted from dynamic testing, and this limitation has been one of the major disadvantages of frequency-based SI methods. However, as shown in Table 2, utilizing additional spectral information can expand data space and, accordingly, can enhance the capability as well as the accuracy of the parameter identification process. For example, if n numbers of natural frequencies are extractable for a given system, one can expand the data space by extracting an additional $(n-1)$ number of antiresonant frequencies and $2 \times (n-1)$ number of SCD frequencies from a single FRF, as shown in Fig. 1. Furthermore, as shown in Table 2, unlike natural frequencies, the values of the

antiresonant and SCD frequencies are different for each and every FRFs. Thus, if a system is complex and consists of more unknown stiffness parameters than the available resonant frequencies, one can further expand the data space by extracting additional antiresonant and SCD frequencies from other FRFs and consequently improve the accuracy of parameter identification process.

6. Conclusions

In this paper, the application of additional spectral information, i.e., antiresonant frequencies and SCD frequencies, to the parameter identification in mechanical problems was presented. The motivation of this study was to investigate the feasibility of utilizing additional spectral information to parameter identification problems and to improve the performance of parameter identification by supplying more information to a sensitivity-based SI technique. The purpose of this study was to extend the sensitivity-based method to accommodate additional spectral information. The performance of utilizing additional spectral information was compared with that of utilizing only natural frequencies via a numerical example of a mechanical system.

From the numerical study, the following observations can be drawn:

1. with additional spectral information such as antiresonant and SCD frequencies, the accuracy of parameter identification can be improved;
2. if the number of spectral pieces of information from FRFs used is equal to or greater than the number of stiffness parameters to be identified, the error in the identified stiffnesses is greatly reduced, regardless of the starting point of the estimated solutions;
3. better parameter identification results were observed to be obtained using the point FRFs than using the transfer FRFs; and
4. the SCD frequencies can be utilized in SI problems.

The simple system presented in the preceding section may not reflect the complexity and uncertainty of real systems; however, the purpose of this paper is to establish the feasibility of the approach. More extensive study on the applicability of the additional spectral information especially to real structures will be addressed in subsequent studies.

References

Choi, S., Stubbs, N., 2004. Damage identification in structures using the time-domain response. Journal of Sound and Vibration 275 (3–5), 577–590.

Collins, J.D., Hart, G.C., Hasselman, T.K., Kennedy, B., 1974. Statistical identification of structures. AIAA Journal 12 (2), 185–190.

D'Ambrogio, W., Fregolent, A., 1998. On the use of consistent and significant information to reduce ill-conditioning in dynamic model updating. Mechanical Systems and Signal Processing 12 (1), 203–222.

Dilena, M., Morassi, A., 2004. The use of antiresonances for crack detection in beams. Journal of Sound and Vibration 276 (1–2), 195–214.

Doebling, S.W., Farrar, C.R., Prime, M.B., Shevitz, D.W., 1996. Damage identification and health monitoring of structural and mechanical systems from changes in their vibration characteristics: a literature review. Technical Report LA-13070-MS, Los Alamos National Laboratory.

Douka, E., Bamnios, G., Trochidis, A., 2004. A method for determining the location and depth of cracks in double-cracked beams. Applied Acoustics 65, 997–1008.

Ewins, D.J., 1984. Modal Testing: Theory and Practice. Research Studied Press Ltd., Hertfordshire, England.

Farrar, C., Jauregui, D., 1996. Damage detection algorithms applied to experimental and numerical modal data from the I-40 bridge. Technical Report LA-13074-MS, Los Alamos National Laboratory.

Friswell, M.I., Mottershead, J.E., 1995. Finite Element Model Updating and Structural Dynamics. Kluwer, Dordrecht, Holland.
Gao, Y., Randall, R.B., 1996. Determination of frequency response functions from response measurements—I. Extraction of poles and zeros from response spectra. Mechanical Systems and Signal Processing 10 (3), 293–317.
Jons, K., Turcotte, J., 2002. Finite element model updating using antiresonant frequencies. Journal of Sound and Vibration 252 (4), 717–727.
Kajiwara, I., Nagamatsu, A., 1993. Optimum design of optical pick-up by elimination of resonance peaks. Journal of Vibration and Acoustics 115, 377–383.
Lallement, G., Cogan, S., 1992. Reconciliation between measured and calculated dynamic behaviors: enlargement of knowledge space. Proceedings of IMAC 10, 487–493.
Lin, R.M., Ewins, D.J., 1994. Analytical model improvement using frequency response functions. Mechanical Systems and Signal Processing 8 (4), 437–458.
Mottershead, J.E., 1990. Theory for the estimation of structural vibration parameters from incomplete data. AIAA Journal 28 (3), 559–561.
Mottershead, J.E., 1998. On the zeros of structural frequency response functions and their sensitivities. Mechanical Systems and Signal Processing 12 (5), 591–597.
Nam, D.H., 2001. Improvements in the accuracy of system identification and nondestructive damage evaluation in civil engineering structures. Ph.D. Dissertation, Texas A&M University, USA.
Rade, D.A., Lallement, G., DaSilva, L.A., 1996. A strategy for the enrichment of experimental data as applied to an inverse eigensensitivity-based F.E. model updating method. Proceedings of IMAC 14, 1078–1085.
Stubbs, N., 1985. A General Theory of Non-destructive Damage Detection in Structures. Structural Control. Martinus Nijhoff Publishers, Dordrecht, Holland, pp. 694–713.
Stubbs, N., Osegueda, R., 1990. Global non-destructive damage evaluation in solids. International Journal of Analytical and Experimental Modal Analysis 2–5, 67–79.
Stubbs, N., Torpunuri, V.S., Lytton, R.L., Magnuson, A.H., 1994. A methodology to identify material properties in pavements modeled as layered viscoelastic halfspaces (Theory). Nondestructive Testing of Pavements and Backcalculation of Moduli, Vol. 2, ASTM STP 1198, pp. 53–67.
Wahl, F., Schmidt, G., Forrai, L., 1999. On the significance of antiresonance frequencies in experimental structural analysis. Journal of Sound and Vibration 219 (3), 379–394.
Zadeh, L.A., 1962. From circuit theory to system theory. Proceeding of IRE 50, 856–865.